MATHEMATICAL BIOSCIENCES
AND ENGINEERING
Volume **1**, Number **1**, June **2004**

http://math.asu.edu/~mbe/

pp. **131–145**

COEXISTENCE IN A METAPOPULATION MODEL WITH EXPLICIT LOCAL DYNAMICS

Zhilan Feng

Department of Mathematics
Purdue University, West Lafayette, IN 47907

Robert Swihart

Department of Forestry and Natural Resources
Purdue University, West Lafayette, IN 47907

Yingfei Yi

School of Mathematics
Georgia Institute of Technology, Atlanta, GA 30332

Huaiping Zhu

Laboratory for Industrial and Applied Mathematics
Department of Mathematics and Statistics
York University, 4700 Keele Street, Toronto, ON M3J 1P3, Canada

(Communicated by Yang Kuang)

Abstract. Many patch-based metapopulation models assume that the local population within each patch is at its equilibrium and independent of changes in patch occupancy. We studied a metapopulation model that explicitly incorporates the local population dynamics of two competing species. The singular perturbation method is used to separate the fast dynamics of the local competition and the slow process of patch colonization and extinction. Our results show that the coupled system leads to more complex outcomes than simple patch models which do not include explicit local dynamics. We also discuss implications of the model for ecological systems in fragmented landscapes.

1. **Introduction.** Destruction and fragmentation of native habitats are widespread and viewed as the most important threats to biodiversity worldwide [31]. Agriculture, urban sprawl, deforestation, and other human activities change the composition and physiognomy of landscapes, often altering individual behavior [24, 33], population dynamics [5], genetic structure [4], and community composition [32] of organisms. Metapopulation models have been used extensively to study the conservation implications of habitat loss and fragmentation. A metapopulation consists of a set of discrete local populations with independent internal dynamics that are linked by dispersal [5]. Metapopulations exist within a network of idealized habitat patches (fragments), occupying some proportion p of these fragments. The original single-species metapopulation model of Levins [13] assumed that changes in patch

2000 *Mathematics Subject Classification.* 92D25 and 34C60 (34E15 37N25 92D40).

Key words and phrases. metapopulation models, competing species, local population dynamics, patch colonization, extinction, fragmented landscapes, ecological systems, singular perturbation.

occupancy were functions solely of colonization rates of empty patches (c) and extinction rates of occupied patches (e). Although overly simplistic, the Levins model provided an essential framework for studies of spatially structured subpopulations linked by dispersal.

In addition to habitat destruction and fragmentation, interspecific competition can be a powerful force structuring local communities [11, 15, 23]. The joint effects of these forces on community structure are of considerable interest, because asymmetric effects of habitat destruction and fragmentation acting on species have the potential to alter outcomes of interactions for competing species. Theoretical models of various types predict that habitat fragmentation may promote coexistence of competing species by permitting inferior competitors to escape spatially by virtue of greater dispersal ability [10, 16, 17].

Unfortunately, metapopulation models generalized to multiple species (e.g., [1, 26, 28, 29]) have failed to incorporate explicitly the local dynamics of species in each patch. An important exception was the model of Hanski and Zhang [7] in which local and metapopulation dynamics were explicitly coupled to enable an examination of the effect of migration on metapopulation persistence. They demonstrated that the use of coupled models can provide insights into conditions for metapopulation persistence that cannot be obtained from simple patch models. In this paper, we generalize the model of Hanski and Zhang's model by including the local dynamics of two weakly competing species. Since local dynamics occur on a much faster time scale than changes in patch occupancy, we can use a singular perturbation argument to separate the model dynamics into two time scales. Our analyses of the slow system show that it is possible for the system to have multiple interior equilibria as well as a unique global interior attractor. When multiple interior equilibria are present, bi-stability may occur, in which case the competing species may stabilize either at an interior equilibrium (both species stably coexist) or at a boundary equilibrium (one species excludes the other species). Finally, we apply the model to a competitive interaction in a fragmented agroecosystem and discuss the implications of our findings for community structure and species conservation.

2. **The model and its fast and slow dynamics.** The Levins model has the form

$$\frac{dp}{dt} = cp(1-p) - ep, \tag{1}$$

where p denotes the proportion of the occupied patches. Its focus is on extinction e and colonization c rates, with no consideration given to the effect of migration on local dynamics. Such an omission may be reasonable when migration rate is low, but if migration rate is high, failure to consider local dynamics may produce models that predict biased results [6]. To study the population-level consequences of local dynamics when migration rates are high, Hanksi and Zhang [7] proposed the following mean-field metapopulation model:

$$\begin{cases} \dfrac{dN}{dt} &= rN\left(1-\dfrac{N}{K}\right) - mN + \alpha mNp, \\ \dfrac{dp}{dt} &= \beta\alpha mNp(1-p) - ep, \end{cases} \tag{2}$$

where p is an element of $[0,1]$ is the fraction of the occupied habitat patches; $N \in [0,\infty)$ is the typical size of existing local populations; $r > 0$ is the average

per capita growth rate due to local births and deaths; $K > 0$ is the average per-patch carrying capacity; $m > 0$ is the per capita emigration rate; $\alpha > 0$ is the fraction of migrating individuals that survived and reached a new patch; $\beta > 0$ is the probability that an arriving individual gives rise to a new local population in an empty patch; and $e > 0$ is the extinction rate of local populations, which is assumed to be independent of N. One scenario fits this description if the extinction is entirely due to environmental causes such as natural disasters, season changes, powerful and fast predation and diseases. This model assumes different time scales for local and metapopulation dynamics and a uniform size for local populations. The model in [7] predicts alternative stable equilibria for parameters in a certain range, and qualitatively different model behaviors are possible when the migration parameter m varies. In [7] they also considered fugitive co-existence by studying an asymmetric competition model in which one competitor is superior (i.e., the inferior species cannot colonize patches occupied by the superior species, and the two competing species cannot co-exist in the same patch).

We generalize the model in [7] by incorporating two competing species that co-exist in the same patch. Let N_1 and N_2 denote the typical local population sizes of the species 1 and 2, respectively, and, let p_1 and p_2 denote the fraction of patches occupied by species 1 and 2, respectively. (We do not required that $p_1 + p_2 \leq 1$.) Because our mean-field formulation focuses on conditions in an average patch, p_1 and p_2 represent measures of landscape occupancy. Assuming competition of the Lotka-Volterra type and using the subscript i to represent the species i, where $i = 1, 2$, we can write the generalized model as follows:

$$\begin{cases} \dfrac{dN_i}{dt} &= r_i N_i \left(1 - \dfrac{N_i}{K_i} - a_{ij}\dfrac{N_j}{K_i}\right) - m_i N_i + \alpha_i m_i N_i p_i, \\ \dfrac{dp_i}{dt} &= \beta_i \alpha_i m_i N_i p_i (1 - p_i) - e_i p_i, \end{cases} \tag{3}$$

where $i, j = 1, 2,\ i \neq j$; a_{ij} is the competition coefficient expressing the per-capita effect of species j on growth rate of species i, and all other parameters are as defined for the model [7]. We adhered to the assumptions of [7] but relaxed the assumption of exclusion of the inferior competitor.

Like Hanski and Zhang, we assume that the changes in p_i occur on a slower time scale than the local population dynamics. Hence, the rate of patch creation by one migrating individual, $\beta_i \alpha_i m_i$, and the rate of patch extinction, e_i, where $i = 1, 2$, are much smaller than all other rates. The smallness of $\beta_i \alpha_i m_i$ can be justified by the fact that β_i is a very small constant because of the low rate of successful colonization of empty patches by one migrating individual (recall that β is the probability that an arriving individual gives rise to a new local population in an empty patch). Therefore, independent of time unit, we can assume that

$$\beta_i = \varepsilon \hat{\beta}_i, \quad e_i = \varepsilon \hat{e}_i, \quad i = 1, 2,$$

where $\varepsilon > 0$ is small. Then system (3) can be rewritten as

$$\begin{cases} \dfrac{dN_i}{dt} &= N_i F_i(N, p_i), \\ \dfrac{dp_i}{dt} &= \varepsilon p_i G_i(N, p_i), \end{cases} \qquad i = 1, 2, \tag{4}$$

where $N = (N_1, N_2)$, and

$$F_i(N, p_i) = r_i\left(1 - \frac{N_i}{K_i} - a_{ij}\frac{N_j}{K_i}\right) - m_i + \alpha_i m_i p_i,$$
$$G_i(N, p_i) = \hat{\beta}_i \alpha_i m_i N_i (1 - p_i) - \hat{e}_i,$$

where $i, j = 1, 2$, and $i \neq j$. Using techniques in singular perturbation theory (see [3, 14]) we can analyze system (4) by analyzing the corresponding fast and slow systems. The fast dynamics of (4) are given by

$$\frac{dN_i}{dt} = N_i F_i(N, p_i), \qquad i = 1, 2. \tag{5}$$

In the fast system (5), p_1 and p_2 are considered as parameters and will be determined later by the slow system. To make the impact of local dynamics transparent, we consider only the scenario in which coexistence of the two species is possible, for which we make the the following assumptions:

$$a_{12}a_{21} < 1, \qquad \delta_i K_i - a_{ij}\delta_j K_j > 0, \qquad i, j = 1, 2,\ i \neq j, \tag{6}$$

where $\delta_i = 1 - (1 - \alpha_i p_i)\frac{m_i}{r_i}$ for $i = 1, 2$. Setting the right hand side of (5) equal to zero, we obtain a unique positive equilibrium $E^* = (N_1^*, N_2^*)$ (a two-dimensional critical manifold, or slow manifold) described by:

$$N_i^* = \frac{1}{1 - a_{12}a_{21}}\left[K_i\left(1 - \frac{m_i}{r_i}(1 - \alpha_i p_i)\right) - a_{ij}K_j\left(1 - \frac{m_j}{r_j}(1 - \alpha_j p_j)\right)\right], \tag{7}$$

where $i, j = 1, 2$, and $i \neq j$. Note that $N_i^* > 0$ under the condition of (6). Let $J(E^*)$ denote the Jacobian at E^*, then

$$\det(J(E^*)) = (1 - a_{12}a_{21})\frac{r_1 r_2 N_1^* N_2^*}{K_1 K_2} > 0,$$

as $a_{12}a_{21} < 1$ and $N_i^* > 0$, where $i = 1, 2$. It follows that E^* is locally asymptotically stable when it exists. Hence, on the fast time scale, all solutions of (3) are hyperbolically asymptotic to the equilibrium E^*, and (7) defines a two-dimensional slow manifold. Re-scaling the time by letting $\tau = t/\varepsilon$ we obtain the following system which governs the slow dynamics:

$$\frac{dp_i}{d\tau} = p_i\left(\hat{\beta}_i \alpha_i m_i N_i^*(1 - p_i) - \hat{e}_i\right), \qquad i = 1, 2, \tag{8}$$

where N_i^* is a function of both p_1 and p_2 (see (7)).

We next focus on the slow dynamics. The trivial equilibrium (extinction), $Q_0 = (p_{10}, p_{20}) = (0, 0)$, always exists. The stability of Q_0 is determined by the relative magnitudes of the patch extinction rate, e_i, and the modified patch colonization rate, c_i:

$$c_i = \frac{\beta_i \alpha_i m_i}{1 - a_{ij}a_{ji}}\left(\left(1 - \frac{m_i}{r_i}\right)K_i - a_{ij}\left(1 - \frac{m_j}{r_j}\right)K_j\right), \tag{9}$$

$i, j = 1, 2,\ i \neq j$. Let

$$\lambda_i = \frac{c_i}{e_i}, \qquad i = 1, 2. \tag{10}$$

Then, Q_0 is stable if

$$\lambda_i < 1, \qquad i = 1, 2, \tag{11}$$

and it is unstable if

$$\lambda_1 > 1 \qquad \text{or} \qquad \lambda_2 > 1. \tag{12}$$

In the standard Lotka-Volterra competition model, or in metapopulation competition models that do not explicitly incorporate local population dynamics [25,28,

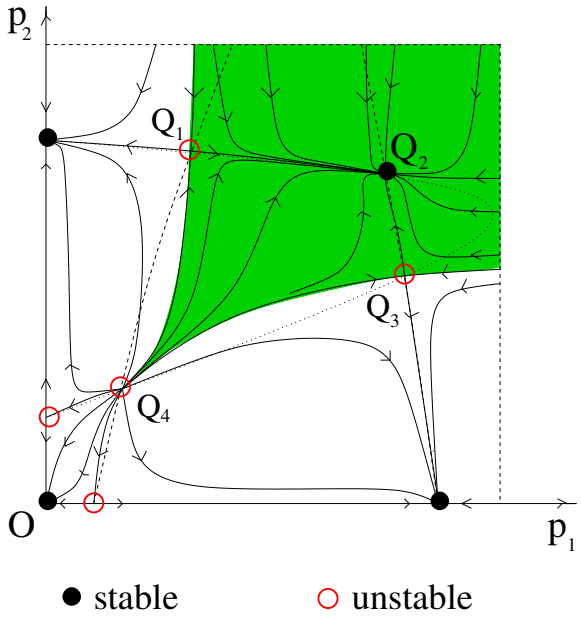

FIGURE 1. There are nine possible equilibria even when $\lambda_i < 1$, where $i = 1, 2$.

29], no stable non-trivial equilibria can exist when the trivial equilibrium is stable. Hence, the two species cannot stably coexist if the extinction equilibrium is stable. This is not the case in our model. For example, (8) may have a stable interior (coexistence) equilibrium even when the parameters satisfy $\lambda_i < 1$, where $i = 1, 2$, which is the stability condition for the trivial equilibrium. In fact, the system (8) may have as many as nine equilibria, as shown in Fig. 1.

The additional condition (besides $\lambda_i < 1$, $i = 1, 2$) that excludes the existence of an interior equilibrium is that at least one of the following two inequalities holds (for a proof see [2]:

$$\left(1 - (1+\alpha_i)\frac{m_i}{r_i}\right) K_i - a_{ij}\left(1 - \frac{m_j}{r_j}\right) K_j > 0, \qquad i, j = 1, 2,\ i \neq j. \tag{13}$$

The condition (13) also can be expressed in terms of the carrying capacities as

$$K_i > f_i(K_j), \qquad i = 1, 2,\ i \neq j, \tag{14}$$

where

$$f_i(K_j) = \frac{a_{ij}\left(1 - \frac{m_j}{r_j}\right) K_j}{1 - (1+\alpha_i)\frac{m_i}{r_i}}, \qquad i, j = 1, 2,\ i \neq j. \tag{15}$$

Although a coexistence equilibrium cannot exist under the conditions (11) and (14), stable non-trivial boundary equilibria (competitive exclusion) may exist when (14) holds for only one value of i. If (14) holds for both $i = 1$ and $i = 2$, then neither non-trivial boundary nor interior equilibria are possible; that is, both species will go extinct. Detailed mathematical proofs of these results are provided in [2]. A stable interior equilibrium is possible when

$$\lambda_1 \geq 1 \qquad \text{and} \qquad \lambda_2 \geq 1, \tag{16}$$

TABLE 1. Possible existence of stable equilibria as λ_i and m_i vary. $\Delta > 0$ is assumed for all cases (see the text). BQ_i denotes (stable) boundary equilibrium on the p_i axis, and IQ denotes (stable) interior equilibrium. Q_0 denotes the trivial equilibrium $(0, 0)$.

	$\lambda_1 \geq 1$	$\lambda_1 < 1,\ K_1 > f_1(K_2)$	$\lambda_1 < 1,\ K_1 < f_1(K_2)$
$\lambda_2 \geq 1$	$BQ_1,\ BQ_2,\ IQ$	$BQ_1,\ BQ_2,\ IQ$	BQ_2
$\lambda_2 < 1,\ K_2 > f_2(K_1)$	$BQ_1,\ BQ_2,\ IQ$	$BQ_1,\ BQ_2,\ IQ$	BQ_2
$\lambda_2 < 1,\ K_2 < f_2(K_1)$	BQ_1	BQ_1	Q_0

or when

$$\lambda_i \geq 1, \quad \lambda_j < 1, \quad K_j > f_j(K_i), \qquad i, j = 1, 2, \quad i \neq j. \tag{17}$$

The condition (16) implies that the modified colonization rates of both species exceeds their respective extinction rates. The condition (17) states that only one species' colonization rate exceeds its extinction rate, but the other species has a carrying capacity that is above the threshold given by (15). Stabilities of various equilibria can be described in terms of λ_i, K_i, and the discriminant, Δ, of a fourth degree polynomial whose positive roots determine the property of interior equilibria; that is, a stable interior equilibrium exists only if $\Delta > 0$. (This polynomial is extremely complex and will not be discussed here–for details see [2].) If we assume $\Delta > 0$ (which is satisfied for the parameter values we use for case studies in section 4), then the dependence of possible stable equilibria on λ_i and K_i is summarized in Table 1. When a stable interior equilibrium exists, it may attract either all solutions with initial values in $\mathbf{D} = \{(p_1, p_2) | 0 < p_1 < 1, 0 < p_2 < 1\}$, or only solutions with initial values in a sub-region of $\mathbf{D}$, in which case an alternative stable (boundary) equilibrium exists. The slow system can have up to 4 interior equilibria in $\mathbf{D} = \{(p_1, p_2) | 0 < p_1 < 1, 0 < p_2 < 1\}$ and up to 9 interior and boundary equilibria for all the choices of positive parameters. The system does not have any closed orbit. Moreover, when there exists a unique interior equilibrium, its attracting area is the whole open unit square; when multiple interior equilibria exist, only one can be stable whose attracting area is only a sub-region of $\mathbf{D}$, in which case a stable boundary equilibrium exists. Some possible cases for coexistence are listed in Fig. 2. We discuss the threshold conditions related to each panel of Fig. 2 in the following section.

3. **The region of stable coexistence.** The following notation will be used in this section:

$$\begin{aligned}
k_i &= a_{ij}\hat{\beta}_i K_j \alpha_i \alpha_j m_i \frac{m_j}{r_j}, \\
\gamma_i &= \frac{1}{a_{ij}\alpha_j K_j \frac{m_j}{r_j}}, \\
k_{i0} &= K_i\big(1 - \frac{m_i}{r_i}\big) - a_{ij}K_j\big(1 - \frac{m_j}{r_j}\big), \qquad i, j = 1, 2,\ i \neq j. \\
k_{i1} &= K_i \alpha_i \frac{m_i}{r_i}, \\
k_{i2} &= \frac{\hat{e}_i(1 - a_{12}a_{21})}{\alpha_i \hat{\beta}_i m_i}.
\end{aligned} \tag{18}$$

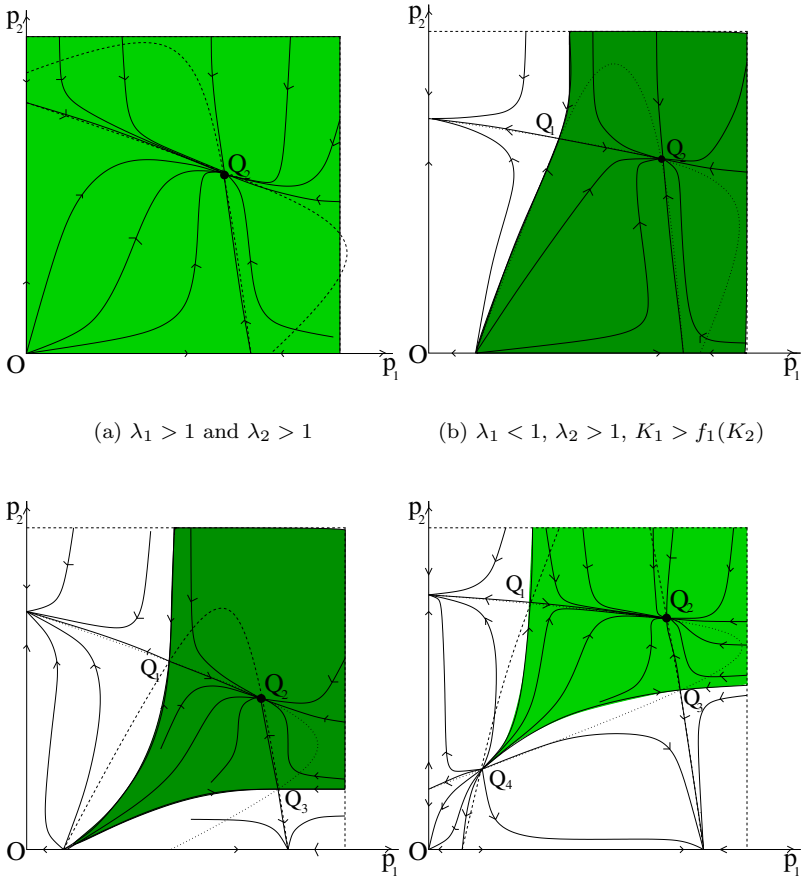

(a) $\lambda_1 > 1$ and $\lambda_2 > 1$

(b) $\lambda_1 < 1$, $\lambda_2 > 1$, $K_1 > f_1(K_2)$

(c) $\lambda_1 < 1$, $\lambda_2 > 1$, $K_1 > f_1(K_2)$

(d) $\lambda_i < 1$, $K_i > f_i(K_j)$, $i, j = 1, 2, i \neq j$

FIGURE 2. Selected scenarios in which a stable coexistence equilibrium exists. In (a), there is a unique interior equilibrium that attracts all solutions. In (b), there are two interior equilibria, one of which is stable. There also is a stable boundary equilibrium on the p_2 axis. In (c), there are three interior equilibria, one of which is stable, and stable boundary equilibria occur on both the p_1 and the p_2 axes. In (d), there are four interior equilibria, one of which is stable. The trivial equilibrium is also stable.

For convenience, we rewrite the slow system (8), with N_i^* replaced by (7), as:

$$p_i' = k_i p_i (1 - p_i)\,(-p_j + h_i(p_i)), \qquad i, j = 1, 2, \qquad i \neq j, \tag{19}$$

where

$$h_i(p_i) = \gamma_i\big(k_{i0} + k_{i1} p_i - \frac{k_{i2}}{1 - p_i}\big). \tag{20}$$

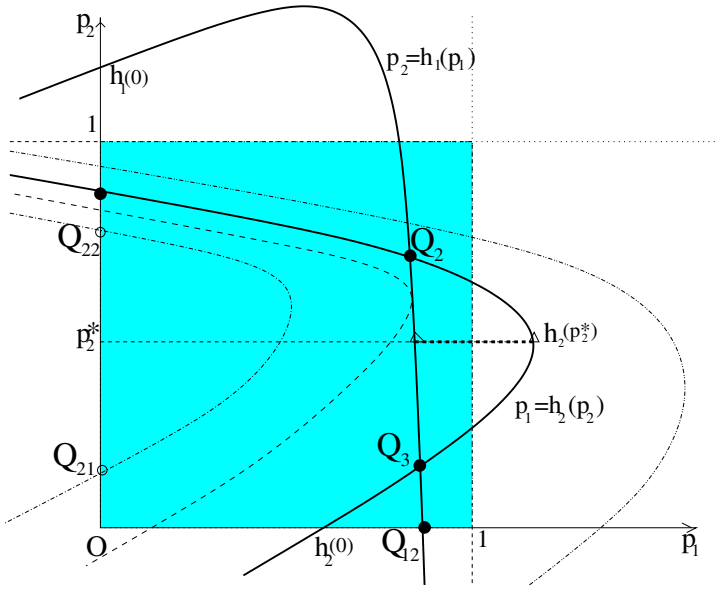

FIGURE 3. The isoclines of the slow system, with some of the boundary and interior equilibria.

The interior equilibria are the intersections of the two isoclines $p_2 = h_1(p_1)$ and $p_1 = h_2(p_2)$. These two isoclines are hyperbolas with two branches and have $p_1 = 1$ and $p_2 = 1$ as a vertical and horizontal asymptote, respectively. Fig. 3 depicts some of the possible cases, and it illustrates that there are up to four possible interior equilibria (intersections of the two curves) when the parameter values change (see also Fig. 2). Only one of these interior equilibria can be stable (Q_2 in Fig. 2 and Fig. 3). As the number of interior equilibria changes, the existence and stability of boundary equilibria also may change, and so does the attraction region of Q_2, which is directly related to the likelihood of coexistence.

It is clear from Fig. 2 that the attraction region of Q_2 is reduced when an alternative stable (boundary) equilibrium exists. Next, we choose the parameter values such that two stable non-trivial equilibria are possible with one interior and the other on the p_1 axis (a similar analysis can be performed if p_1 is replaced by p_2). This leads to the following assumption:

ASSUMPTION 1. $K_1 < K_2$, $a_{12} > a_{21}$, $m_1 \geq m_2$, $r_1 > r_2$, $\alpha_1 \leq \alpha_2$, $\hat{\beta}_1 \geq \hat{\beta}_2$.

We will fix all parameters except K_2 and $\hat{e}_2$, which will be our bifurcation parameters. Let

$$K_{2max} = \frac{K_1(1 - \frac{m_1}{r_1}) - \dfrac{\hat{e}_1(1 - a_{12}a_{21})}{\alpha_1\hat{\beta}_1 m_1}}{a_{12}\left[1 - (1 - \alpha_2)\frac{m_2}{r_2}\right]}. \tag{21}$$

Then we can verify that $K_2 < K_{2max}$ implies $h_1(0) > 0$. In this case, as shown in Fig. 3, the isocline $p_2 = h_1(p_1)$ and the p_1 axis share a unique intersection at $Q_{12} = (p_{12}, 0)$ with $p_{12} \in (0, 1)$, which is the unique nontrivial boundary equilibrium on the p_1 axis. Thus, in the rest of this section we assume that

ASSUMPTION 2. $0 < K_2 < K_{2max}$.

From the results in [2], we know that Q_{12} moves towards the origin as K_2 increases (subject to the constraint $K_2 < K_{2max}$) and that the slow system has at most two interior equilibria for $K_2 \in (0, K_{2max})$.

Next we discuss how the equilibria and their stabilities change with K_2 and $\hat{e}_2$. Notice that an equilibrium on the p_2-axis satisfies $h_2(p_2) = 0$, or equivalently,

$$k_{21}p_2^2 + (k_{20} - k_{21})p_2 + k_{22} - k_{20} = 0. \tag{22}$$

Let

$$\begin{aligned}\Delta_2 &= (k_{20} - k_{21})^2 - 4k_{21}(k_{22} - k_{20}) \\ &= \left[-a_{21}K_1\big(1 - \frac{m_1}{r_1}\big) + K_2\big(1 - (1+\alpha_1)\frac{m_2}{r_2}\big)\right]^2 - \frac{4\hat{e}_2(1 - a_{21}a_{12})}{r_2\hat{\beta}_2}K_2.\end{aligned}$$

Then Equation (22) has either two solutions if $\Delta_2 > 0$ or no solutions if $\Delta_2 < 0$. Solving the quadratic equation $\Delta_2 = 0$ in terms of K_2, we get

$$K_2 = c_{20} + c_{21}\hat{e}_2 + c_{21}\sqrt{\hat{e}_2^2 + c_{22}\hat{e}_2}, \tag{23}$$

where

$$\begin{aligned}c_{20} &= \frac{a_{21}K_1(1 - \frac{m_1}{r_1})}{1 - (1-\alpha_2)\frac{m_2}{r_2}}, \\ c_{21} &= \frac{2(1 - a_{12}a_{21})}{r_2\hat{\beta}_2[1 - (1-\alpha_2)\frac{m_2}{r_2}]^2}, \\ c_{22} &= \frac{r_2\hat{\beta}_2 a_{21}K_1(1 - \frac{m_1}{r_1})[1 - (1-\alpha_2)\frac{m_2}{r_2}]}{1 - a_{12}a_{21}}.\end{aligned}$$

The right-hand side of (23) defines a function of $\hat{e}_2$, which determines a curve of saddle-node bifurcation. We denote this function by $K_{2sn1}(\hat{e}_2)$ (sn designates saddle-node bifurcation). Hence, as K_2 increases through K_{2sn1}, a saddle-node bifurcation occurs, and there are two equilibria on the p_2 axis (Fig. 3). These two equilibria are denoted by $Q_{21} = (0, p_{21})$ and $Q_{22} = (0, p_{22})$, where $0 < p_{21} < p_{22} < 1$ are the two roots of $h_2(0)$ determined by Equation (22).

As K_2 continues to increase (subject to the constraint $K_2 < K_{2sn1} < K_{2max}$), the isocline $p_1 = h_2(p_2)$ on the far left (one of the dashed curves in Fig. 3) shifts to the right, and when it intersects with the isocline $p_2 = h_1(p_1)$, the interior equilibria appear (the solid curves). To locate this bifurcation curve, we notice that $p_1 = h_2(p_2)$ has a local minimum at

$$p_2^* = 1 - \frac{1}{\alpha_2 m_2}\sqrt{\frac{r_2\hat{e}_2(1 - a_{12}a_{21})}{\hat{\beta}_2 K_2}}.$$

This allows for another saddle-node bifurcation when $p_2^* = h_1\left(h_2(p_2^*)\right)$, which defines the bifurcation curve

$$K_2 = K_{2sn2}(\hat{e}_2) \tag{24}$$

in the positive quadrant (see Fig. 3 and Fig. 4). Hence, there are no interior equilibria for $0 < K_2 < K_{2sn2}$. As K_2 increases and crosses the curve $K_2 = K_{2sn2}$, two equilibria Q_2 and Q_3 appear in the interior of $\mathbf{D}$ through a saddle-node bifurcation. It is shown in [2] that Q_2 is an attracting node and that Q_3 is a saddle point.

Another saddle-node bifurcation occurs when the equilibrium Q_{21} on the p_2 axis moves downward and passes through the origin, which occurs at $h_2(0) = 0$ (Fig. 3),

or

$$K_2 = K_{2sn3}(\hat{e}_2) = \frac{a_{21}K_1(1-\frac{m_1}{r_1})}{1-\frac{m_2}{r_2}} + \frac{(1-a_{12}a_{21})\hat{e}_2}{\alpha_2\hat{\beta}_2 m_2(1-\frac{m_2}{r_2})}. \tag{25}$$

Hence, when K_2 increases and passes K_{2sn3}, the number of nontrivial boundary equilibria on the p_2 axis changes from two to one (Fig. 4). An ecological consequence of this change is an increase of the attraction region of the stable coexistence equilibrium.

If K_2 continues to increase, the interior equilibrium Q_3 will coalesce with Q_{12} on the p_1 axis and move out of the region $\mathbf{D}$ through another saddle-node bifurcation. The bifurcation curve is determined by $h_1(h_2(0)) = 0$. Solving this equation for K_2 we get

$$K_2 = K_{2sn4}(\hat{e}_2) = d_{20} + d_{21}\hat{e}_2 + d_{22}\sqrt{\hat{e}_2^2 + d_{23}\hat{e}_2 + d_{24}} \tag{26}$$

where

$$\begin{aligned}
d_{20} &= \frac{a_{21}K_1[1-(1-\alpha_1)\frac{m_1}{r_1}]}{2(1-\frac{m_2}{r_2})},\\
d_{21} &= \frac{1-\frac{1}{2}a_{12}a_{21}}{\alpha_2\hat{\beta}_2 m_2(1-\frac{m_2}{r_2})},\\
d_{22} &= \frac{a_{12}a_{21}}{2\alpha_2\hat{\beta}_2 m_2(1-\frac{m_2}{r_2})},\\
d_{23} &= -\frac{2}{a_{12}}K_1\alpha_2\hat{\beta}_2 m_2[1-(1-\alpha_1)\frac{m_1}{r_1}],\\
d_{24} &= \frac{(\alpha_2\hat{\beta}_2 m_2)^2}{r_1\hat{\beta}_1 a_{12}^2}\left[r_1\hat{\beta}_1(1-(1-\alpha_2)\frac{m_2}{r_2})^2K_1^2 - 4\hat{e}_1K_1\right].
\end{aligned}$$

When K_2 increases and passes K_{2sn4}, the number of nontrivial interior equilibria changes from two to one and the attraction region of the stable coexistence equilibrium further increases.

Finally, for $K_{2sn4} < K_2 < K_{2max}$, the slow system has a unique interior equilibria Q_2 that is attracting (Fig. 4).

We summarize the above results in the following theorem and in Fig. 4.

THEOREM 1. *Let Assumptions 1 and 2 hold. For any fixed $\hat{e}_2 > 0$ and $K_2 \in (0, K_{2max})$, the slow system (19) undergoes four saddle-node bifurcations along the curves in the $(\hat{e}_2, K_2)$ plane: (i) $K_2 = K_{2sn1}(\hat{e}_2)$ is unstable, and the bifurcation occurs on the p_2-axis; (ii) $K_2 = K_{2sn2}(\hat{e}_2)$ is stable, and the bifurcation occurs in the interior of $\mathbf{D}$; (iii) $K_2 = K_{2sn3}(\hat{e}_2)$ is unstable, and the bifurcation occurs at the origin; and (iv) $K_2 = K_{2sn4}(\hat{e}_2)$ is stable, and the bifurcation occurs on the p_1-axis. Moreover, the system (19) has*

a. *a unique stable boundary equilibrium, Q_{12}, on the p_1-axis for $0 < K_2 < K_{2sn1}$;*
b. *two boundary equilibria, Q_{21} and Q_{22}, on the p_2-axis for $K_{2sn1} < K_2 < K_{2sn2}$, with Q_{22} being a saddle and Q_{21} being a repelling node;*
c. *two interior equilibria, Q_2 and Q_3, for $K_{2sn2} < K_2 < K_{2sn3}$, with Q_2 being a stable node and Q_3 being a saddle point;*
d. *two interior equilibria, Q_2 and Q_3, as in (c) and two boundary equilibria, Q_{12} and Q_{22}, for $K_{2sn3} < K_2 < K_{2sn4}$, with Q_{12} being a stable node and Q_{22} being a saddle point;*
e. *a unique attracting interior equilibria, Q_2, and two boundary equilibria, Q_{12} and Q_{22}, for $K_{2sn4} < K_2 < K_{2max}$, with both boundary equilibria being saddle points.*

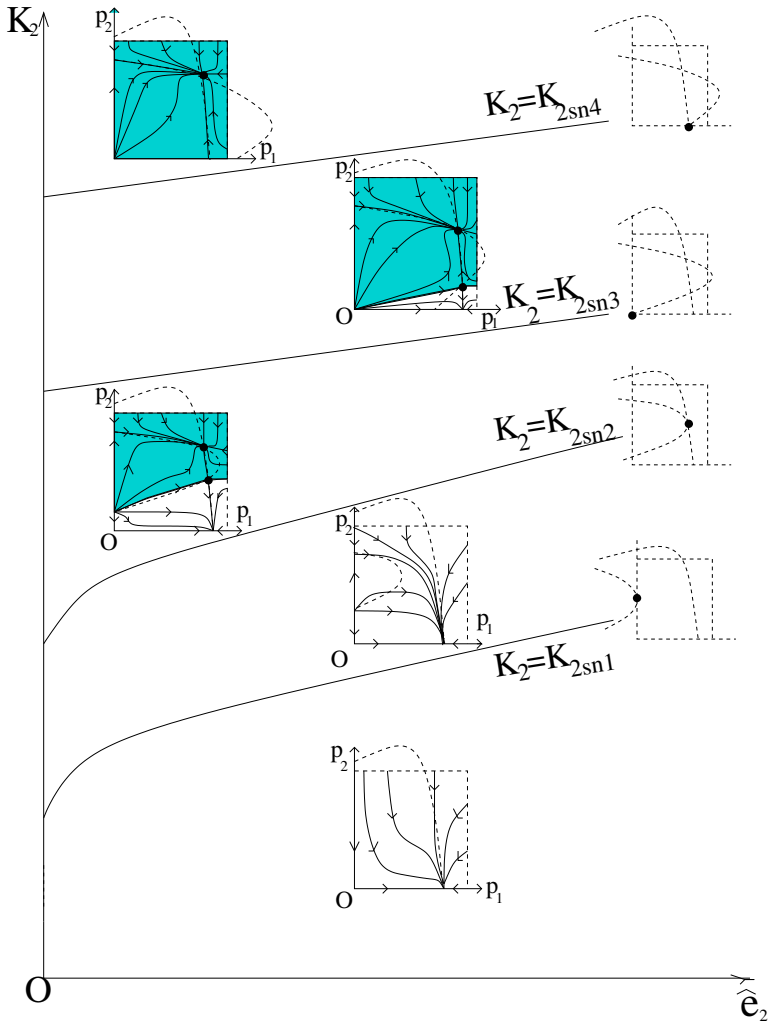

FIGURE 4. Bifurcation curves using $\hat{e}_2$ and K_2) as bifurcation parameters.

4. **Case study.** The results in Theorem 1 can provide useful insights into ecological consequences resulting from changes in parameters governing the system. As an example, we consider the potential dynamics of two species of rodents, *Peromyscus leucopus* (white-footed mouse) and *Tamias striatus* (Eastern chipmunk), that occupy remnant forest patches in the central United States. Our studies of the species in Indiana have revealed that they rely upon a common core food resource [12, 27] and exhibit weak levels of competition in which *T. striatus* is dominant [21]. However, *T. striatus* is more sensitive to the effects of forest fragmentation than *P. leucopus* and typically occurs at lower densities [9, 19]. Thus, this system can provide a useful illustration of the potential effects of varying levels of habitat loss and extinction risk on the outcome of competition.

Using our knowledge of this system, we assigned the following set of realistic parameter values to observe numerically (using MAPLE) the quantitative changes to the attracting region of the stable coexistence equilibrium. In all that follows,

TABLE 2. The bifurcation values for the four cases

	Case 1: $\hat{e}_2 = 4$	**Case 2**: $\hat{e}_2 = 2.5$	**Case 3**: $\hat{e}_2 = 1$	**Case 4**: $\hat{e}_2 = 0.2$
K_{2max}	223	515	696	7012
K_{2sn4}	91	102	99	839
K_{2sn3}	89	97	93	775
K_{2sn2}	86	87	72	416
K_{2sn1}	85	84	68	385

species 1 is the inferior competitor (*P. leucopus*) and species 2 is the superior competitor (*T. striatus*):

$$\begin{array}{llll} r_1 = 0.7, & m_1 = 0.1, & \alpha_1 = 0.5, & \beta_1 = 0.05, \\ r_2 = 0.15, & m_2 = 0.1, & \alpha_2 = 0.6, & \beta_2 = 0.03, \\ a_{12} = 0.5, & a_{21} = 0.1 & & \end{array} \tag{27}$$

Note that the relative locations of the bifurcation curves described in Theorem 1 are dependent on other parameter values, including K_1 and $\hat{e}_1$. We considered four cases corresponding to the following four sets of K_1 and $\hat{e}_1$:

1. $K_1 = 100$, and $\hat{e}_1 = 1$
2. $K_1 = 225$, and $\hat{e}_1 = 1$
3. $K_1 = 300$, and $\hat{e}_1 = 0.5$
4. $K_1 = 3000$, and $\hat{e}_1 = 0.1$

These cases correspond to decreasing severity of habitat fragmentation and extinction risk. In many parts of the midwestern United States, a carrying capacity of 100 for *P. leucopus* (case 1) represents a situation in which each forest remnant is only 0.1 to 3 ha in size [18]. The density of *P. leucopus* declines nonlinearly as forest patch area increases [18, 20], with the result that average patch sizes for cases 2 through 4 are roughly 5 to 15 ha, 10 to 20 ha, and 100 to 300 ha, respectively.

The bifurcation curves for all four cases were computed using MAPLE and are shown in Fig. 5. Clearly, the mouse-chipmunk system shows the same qualitative properties as that in Fig. 4. Several points on the bifurcation curves are listed in Table 2. For example, if $K_1 = 300$, $\hat{e}_1 = 0.5$ (case 3) and $\hat{e}_2 = 1$, then $K_{2sn4} = 99$ and $K_{2sn2} = 72$. Hence, according to Theorem 1, for $K_2 > 99$, the attracting region of the stable interior equilibrium is the entire interior of $\mathbf{D}$ (coexistence is expected for all initial data), whereas for $72 < K_2 < 99$, there exists a stable boundary equilibrium on the p_1 axis that attracts solutions with initial data in the unshaded part of $\mathbf{D}$ (competitive exclusion of species 2). For $K_2 < 72$, coexistence is impossible and species 2 will always suffer extinction, despite its competitive superiority. A notable pattern from this example is the narrow range over which coexistence thresholds occur when carrying capacity (and hence forest patch size) is small. In highly fragmented landscapes characterized by small patches with low carrying capacities, slight changes in K_2 or $\hat{e}_2$ can make the difference between coexistence and competitive exclusion. For *T. striatus*, local carrying capacities are approximately 35, 100, 225, and 3000 for cases 1 through 4, respectively [19]. Possible positions for cases 1 and 2 are shown in Fig. 5 (the positions for cases 3 and 4 are far above all four curves and are not shown). Thus, competitive coexistence becomes increasingly likely as forest patch size increases. We do not have reliable estimates for background extinction rates in this system, but the values used in Table 2 are illustrative of the process. For a landscape, with extremely small patches (case

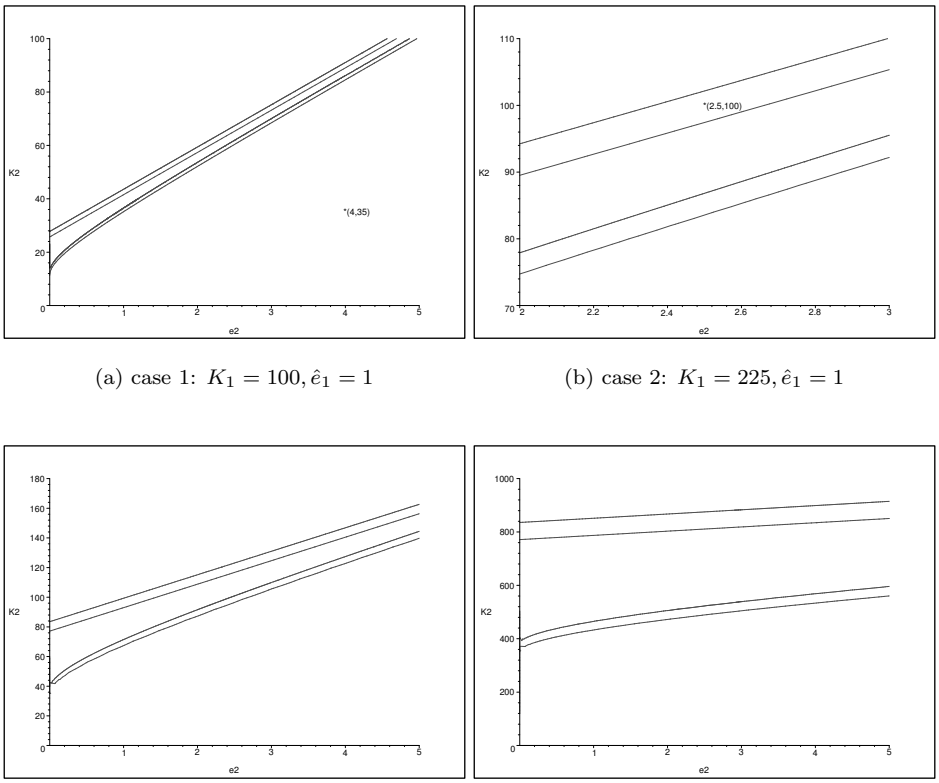

(a) case 1: $K_1 = 100, \hat{e}_1 = 1$

(b) case 2: $K_1 = 225, \hat{e}_1 = 1$

(c) case 3: $K_1 = 300, \hat{e}_1 = 0.5$

(d) case 4: $K_1 = 3000, \hat{e}_1 = 0.1$

FIGURE 5. Bifurcation curves for the four cases.

1), *T. striatus* is predicted to suffer extinction despite its competitive advantage. A slight increase in patch size (case 2) may lead to stable coexistence, albeit in a subset of the interior of **D** (Fig. 5). For large patches with correspondingly large carrying capacities, stable coexistence is predicted for all occupancy levels (Fig. 5).

5. **Conclusions.** Our model demonstrates the importance of considering local patch dynamics when attempting to understand the behavior of metacommunities structured partly by competition. A focus solely on colonization and extinction processes fails to capture the rich dynamics associated with systems that are affected by weak competition. Moreover, the interplay between local- and landscape-level processes can lead to counter intuitive results and multiple stable equilibria not predicted by models that ignore either colonization dynamics or competitive interactions. Conservation considerations in fragmented landscapes frequently fail to consider the influence of interspecific interactions on persistence. Our model results suggest that failure to account for competitive interactions may lead to biased predictions regarding persistence of species, and these considerations may be especially important as habitat loss and fragmentation intensify.

For decades, competition was touted by ecologists as a dominant force structuring local communities (reviewed in [22]). More recently, the role of spatial structure has been increasingly acknowledged as an important predictor of local community structure in fragmented landscapes (e.g., [8, 30]). By considering jointly the effects of competition and spatial structure within the context of analytical models such as the one developed in this paper, ecologists may be empowered with the tools needed for a more complete understanding of communities in complex landscapes.

Acknowledgments. The research of Feng was supported in part by James S. McDonnell Foundation grant JSMF-220020052 and by NSF grant DMS-0314575. The research of Yi was supported in part by NSF grant DMS-0204119. The research of Zhu was supported in part by Natural Sciences and Engineering Research Council (NSERC) and by Canada Foundation for Innovation (CFI). Support for our research was also provided by NSF grant SES-0119908 and by Environmental Sciences and Engineering Institute at Purdue (to RKS and ZF).

REFERENCES

[1] Bascompte, J. and Sole, R. V. (1998). Effects of habitat destruction in a prey-predator metapopulation model. *J. Theor. Biol.* **195**, 383–393.
[2] Feng, Z-L., Yi, Y-F. and Zhu, H-P. (2003). Metapopulation Dynamics with migration and local competition. Fields Institute Communication, *AMS* **36**, 119–135.
[3] Fenichel, N (1979). Geometric singular perturbation theory for ordinary differential equations. *J. Diff. Eqn.* **31**, 53–98.
[4] Gaines, M. S., Diffendorfer, J. E. , Tamarin, R. H. and Whittam, T. S. (1997). The effects of habitat fragmentation on the genetic structure of small mammal populations. *Journal of Heredity* **88**, 294–304.
[5] Hanski, I (1998). Metapopulation Dynamics. *Nature* **396**, 41–49.
[6] Hanski, I (1999). Metapopulation Ecology. Oxford University Press.
[7] Hanski, I. and Zhang, D. (1993). Migration, metapopulation dynamics and fugitive co-existence. *J. Theor. Biol.* **163**, 491–504.
[8] Harrison, S. (1999). Local and regional diversity in a patchy landscape: Native, alien, and endemic herbs on serpentine. *Ecology* **80**, 70–80.
[9] Henein, K., Wegner, J. and Merriam, G. (1998). Population effects of landscape model manipulation on two behaviourally different woodland small mammals. *Oikos* **81**, 168–186.
[10] Holmes, E. E. and Wilson, H. B. (1998). Running from trouble: long-distance dispersal and the competitive coexistence of inferior species. *American Naturalist* **151**, 578–586.
[11] Hopf, F. A., Valone, T. J. and Brown, J. H. (1993). Competition theory and the structure of ecological communities. *Evolutionary Ecology* **7**, 142–154.
[12] Ivan, J. S., and Swihart, R. K. (2000). Selection of mast by granivorous rodents of the central hardwood forest region. *Journal of Mammalogy* **81**, 549–562.
[13] Levins, R (1969). Some demographic and genetic consequences of environmental heterogeneity for biological control. *Bull. Entom. Soc. Am.* **15**, 237–240.
[14] O'Malley, R. E. Jr (1974). Introduction to Singular Perturbations. Academic Press, New York.
[15] McIntosh, R. P (1995). H. A. Gleason's 'individualistic concept' and theory of animal communities: a continuing controversy. *Biological Review* **70**, 317–357.
[16] Moilanen, A. and Hanski, I. (1995). Habitat destruction and coexistence of competitors in a spatially realistic metapopulation. *Journal of Animal Ecology* **64**, 141–144.
[17] Nee, S. and May, R. M. (1992). Dynamics of metapopulations: habitat destruction and competitive coexistence. *Journal of Animal Ecology* **61**, 37–40.
[18] Nupp, T. E. and Swihart, R. K. (1996). Effect of forest patch area on population attributes of white-footed mice (Peromyscus leucopus) in fragmented landscapes. *Canadian Journal of Zoology* **74**, 467–472.

[19] Nupp, T. E. and Swihart, R. K. (1998). Influence of forest fragmentation on population attributes of white-footed mice and eastern chipmunks. *Journal of Mammalogy* **79**, 1234–1243.

[20] Nupp, T. E. and Swihart, R. K. (2000). Landscape-level correlates of small mammal assemblages in forest fragments of farmland. *Journal of Mammalogy* **81**, 512–526.

[21] Nupp, T. E. and Swihart, R. K. (2001). Assessing competition between forest rodents in a fragmented landscape of midwestern USA. *Mammalian Biology* **66**, 345–356.

[22] Schluter, D. and Ricklefs, R. E. (1993). Species diversity: an introduction to the problem. Pages 1-10 in R. E. Ricklefs and D. Schluter (editors), Species diversity in ecological communities. Historical and geographical perspectives. University of Chicago Press, Chicago.

[23] Schoener, T. W. (1983). Field experiments on interspecific competition. *American Naturalist* **122**, 240–285.

[24] Sheperd, B. F. and Swihart, R. K. (1995). Spatial dynamics of fox squirrels (Sciurus niger) in fragmented landscapes. *Canadian Journal of Zoology* **73**, 2098–2105.

[25] Slatkin, M. (1974). Competition and regional coexistence. *Ecology* **55**, 128–134.

[26] Swihart, R. K., Feng, Z-L., Slade, N. S., Doran, D. M. and Gehring, T. M. (2001). Effects of habitat destruction and resource supplementation in a predator-prey metapopulation model. *J. Theor. Biol.* **210**, 287–303.

[27] Swihart, R. K., Gehring, T. M., Kolozsvary, M. B. and Nupp, T. E.(2003). Responses of resistant vertebrates to habitat loss and fragmentation: the importance of niche breadth and range boundaries. *Diversity and Distributions* **9**, 1–18.

[28] Taneyhill, D. E. (2000). Metapopulation dynamics of multiple species: the geometry of competition in a fragmented habitat. *Ecological Monographs* **70**, 495–516.

[29] Wang, Z-L., Wang, F-Z, Chen, S. and Zhu, M-Y. (2002). Competition and coexistence in regional habitats. *American Naturalist* **159**, 498–508.

[30] Wilson, D. S. (1992). Complex interactions in metacommunities, with implications for biodiversity and higher levels of selection. *Ecology* **73**, 1984–2000.

[31] Wilcox, B. A. and Murphy, D. D. (1985). Conservation strategy: the effects of fragmentation on extinction. *American Naturalist* **125**, 879–887.

[32] Wright, D. H., Patterson, B. D., Mikkelson, G. M., Cutler, A. and Atmar, W. (1998). A comparative analysis of nested subset patterns of species composition. *Oecologia* **113**, 1–20.

[33] Zollner, P. A (2000). Comparing the landscape level perceptual abilities of forest sciurids in fragmented agricultural landscapes. *Landscape Ecology* **15**, 523–533.

Received on Feb. 20, 2004. Revised on March 7, 2004.

E-mail address: zfeng@math.purdue.edu
E-mail address: rswihart@fnr.purdue.edu
E-mail address: yi@math.gatech.edu
E-mail address: huaiping@mathstat.yorku.ca